Non-homogeneous SiGe-on-insulator formed by germanium condensation process[*]

Huang Shi-Hao(黄诗浩), Li Cheng(李 成)[†], Lu Wei-Fang(卢卫芳), Wang Chen(王 尘),
Lin Guang-Yang(林光杨), Lai Hong-Kai(赖虹凯), and Chen Song-Yan(陈松岩)

Department of Physics, Semiconductor Photonics Research Center, Xiamen University, Xiamen 361005, China

Ge condensation process of a sandwiched structure of Si/SiGe/Si on silicon-on-insulator (SOI) to form SiGe-on-insulator (SGOI) substrate is investigated. The non-homogeneity of SiGe on insulator is observed after a long time oxidation and annealing due to an increased consumption of silicon at the inflection points of the corrugated SiGe film morphology, which happens in the case of the rough surface morphology, with lateral Si atoms diffusing to the inflection points of the corrugated SiGe film. The transmission electron microscopy measurements show that the non-homogeneous SiGe layer exhibits a single crystalline nature with perfect atom lattice. Possible formation mechanism of the non-homogeneity SiGe layer is presented by discussing the highly nonuniform oxidation rate that is spatially dependent in the Ge condensation process. The results are of guiding significance for fabricating the SGOI by Ge condensation process.

1. Introduction

Si/Ge heterostructures on SiGe-on-insulator (SGOI) or Ge-on-insulator (GOI) structures are one of the most promising substrates for advanced heterogeneous integration of various functional devices including Si-based optoelectronic integrated circuits and Ge metal–oxide-semiconductor field-effect transistors.[1–5] To date, there have been two key methods to fabricate SGOI or GOI substrate, one is the wafer bonding technology,[6] and the other is germanium condensation technology.[7] Actually, the latter way is a promising approach compatible with complementary metal–oxide semiconductor (CMOS) technology. Germanium condensation process involves a selective Si oxidation of a SiGe layer epitaxially grown on a silicon-on-insulator (SOI) wafer in a dry atmosphere at high oxidation temperature.

Although much work on germanium condensation process has been reported already,[8–15] the behavior of the selective oxide of silicon process still needs further study, such as the formation of non-homogeneity SiGe layer in germanium condensation process. Balakumar *et al.*[11,16] observed the SiGe amorphization during the undesired consequence of lowering of oxidation temperature for Ge condensation and the amorphous/crystalline SiGeO formation with/without intermittent SiO_2 etching during the Ge condensation. Gunji *et al.*[7] found that the strain relaxation of the SiGe layer occurred due to both intrinsic stacking fault formation and biaxial stress-driven buckling of the SiGe layers through viscous flow of the overlying and underlying SiO_2 layers during high temperature oxidation and annealing. In our earlier reports,[18–20] we investigated the strain relaxation in ultrathin SGOI substrates fabricated by multistep Ge condensation method and the GOI substrate with large biaxial tensile strain was successfully fabricated. However, the mechanism of the non-homogeneous SiGe layer formation in the Ge condensation process remains elusive.

In this paper, we report on the non-homogeneous SGOI fabricated by Ge condensation technology. The surface morphology, strain relaxation, and crystallinity of the film in the Ge condensation process are systematically characterized. Possible formation mechanism of the non-homogeneous SiGe layer is presented.

2. Experimental procedures

SOI wafer with a 50-nm top Si layer and a 375-nm BOX layer, fabricated by SIMOX technology, was cleaned using a standard RCA cleaning procedure before being loaded into the ultrahigh vacuum growth chamber. Before growing, the substrate was baked at 850 °C for 30 min to deoxidize. A 15-nm Si buffer layer was grown on the SOI substrate at 600 °C, followed by about 100-nm $Si_{0.58}Ge_{0.42}$ epilayer with a 5-nm Si cap layer to avoid the formation of GeO, mixed $(Si,Ge)O_2$, or SiO_2–GeO_2 during the first oxidation stages.[21] The degree of strain relaxation of the as-grown sample is 68% determined by Raman spectroscopy and double-crystal X-ray diffraction

http://iopscience.iop.org/cpb   http://cpb.iphy.ac.cn

measurement. Then the epitaxially grown wafer was cleaved into several pieces and oxidized or annealed in the conventional tube furnace in a pure O_2 or N_2 environment. The schematic diagram of the Ge condensation process is shown in Fig. 1. The typical samples with various Ge content values in the Ge condensation processes were denoted as samples A, B, C, and D. The oxidation and annealing temperature were both chosen to be below the melting point of $Si_{1-x}Ge_x$. Samples underwent the initial cyclic oxidation (30 min)/annealing (30 min) process at 1050 °C for 4 cycles, denoted as sample A. The second cyclic oxidation (30 min)/annealing (30 min) was performed at 1150 °C for 4 cycles, denoted as sample B. After that, the temperature was reduced to 900 °C with 12 and 18 cycles of oxidation/annealing (denoted as samples C and D), respectively. The strain status and Ge content values in the SiGe layers were evaluated by Raman spectroscopy. The surface morphologies of the samples with the oxide removed were analyzed by atomic force microscopy (AFM).
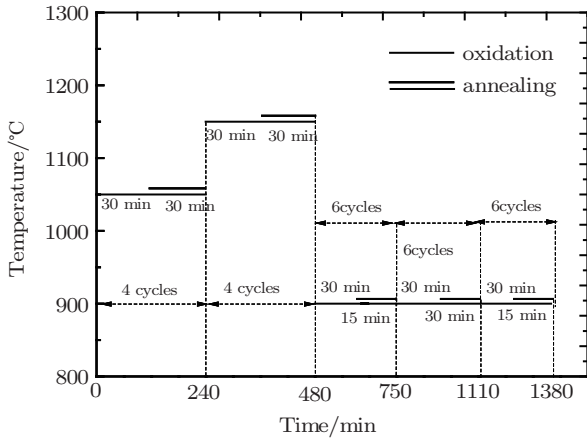

Fig. 1. Schematic diagram of the Ge condensation process. The oxidation and annealing temperature are both under the melting point of the $Si_{1-x}Ge_x$ layer.

3. Results and discussion

Raman spectra are employed to evaluate the values of Ge content and strain in the SiGe layers. Figure 2 shows a series of the Raman spectra for various oxidation and annealing times, using a 532-nm laser as excitation source. There are four distinct peak positions: Si–Si mode in Si substrate at ~ 520.6 cm^{-1}, Si–Si mode in the SiGe layers at ~ 500 cm^{-1}, Si–Ge mode in the SiGe layers at ~ 400 cm^{-1}, and the leftmost peak corresponding to the Ge–Ge mode in the SiGe layers at ~ 300 cm^{-1}. For sample A, after being oxidized and annealed at 1050 °C, there are a weakly defined peak belonging to the Ge–Ge mode in the SiGe layer and two other clear peaks due to the Si–Si and Si–Ge peak modes, in addition to the strong Si–Si mode in Si substrate. As the Ge condensation proceeds, the signals of Si–Si modes in the SiGe layer begin to decrease and the peak of the Ge–Ge mode near 300 cm^{-1} becomes stronger, while the peak of the Si–Ge mode in the

SiGe layer increases with oxidation time at the beginning and then decreases when the Ge content value is higher than 0.5.
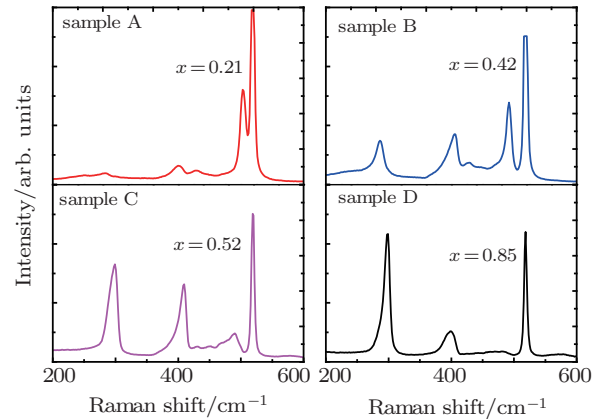

Fig. 2. (color online) A series of the typical Raman spectra for different oxidation and annealing times, using a 532-nm laser as excitation source.

From the Raman spectra, the values of Ge content and strain in the SiGe layers can be determined: (i) when the intensity of Si–Si peak in the SiGe layer is larger than those of Si–Ge and Ge–Ge peaks and it is suggested that Ge content value should be less than 0.5 in the SiGe layer, the values of Ge content and strain in the SiGe layers are evaluated from the peak positions of Si–Si and Si–Ge modes in the SiGe layers from the following equations:[22]

$$\omega_{Si-Si} = 520.6 - 62x - 815\varepsilon_{11},$$
$$\omega_{Si-Ge} = 400.5 + 14.2x - 575\varepsilon_{11}, \tag{1}$$

where ω_{Si-Si} and ω_{Si-Ge} are the Raman shifts of Si–Si and Si–Ge peaks in the $Si_{1-x}Ge_x$ layer respectively; x and ε_{11} are the values of content and in-plane residual strain in the $Si_{1-x}Ge_x$ alloy, respectively. (ii) When the intensity of Ge–Ge peak in the SiGe layer is much stronger than that of Si–Si peak, indicating that Ge content is larger than 0.5, the values of Ge content and strain in the SiGe layer can be calculated from the ratio of the integrated intensity between the peaks of Si–Ge and Ge–Ge modes in the $Si_{1-x}Ge_x$ layers by the equation[22]

$$\frac{I_{Ge-Ge}}{I_{Si-Ge}} = \frac{Bx}{2(1-x)}, \tag{2}$$

where I_{Ge-Ge} and I_{Si-Ge} are the intensities of Ge–Ge and Si–Ge mode fitted by Gaussian distribution, respectively. The coefficient B is determined to be 1 for our Raman experimental setup at 532-nm excitation wavelength using the XRD data available from a number of samples as shown in our previous reports.[18,23] The calculated results indicate that the values of residual strain in the SiGe layer in all of the oxidized samples are nearly zero, which implies that the SiGe layer is nearly fully relaxed in the Ge condensation process.

In Fig. 3, the scatters with errors of ± 0.01 are the summary of Raman measurements of the dependence of the optic mode frequency on the content x in the $Si_{1-x}Ge_x$ layer, and

the solid lines represent the content x-dependent frequencies for the three optic modes in the fully relaxed $Si_{1-x}Ge_x$ alloy system reported in Refs. [24] and [25]. It is revealed that the SiGe layers are already fully relaxed in the Ge condensation process, which coincides with the calculated results as suggested previously.
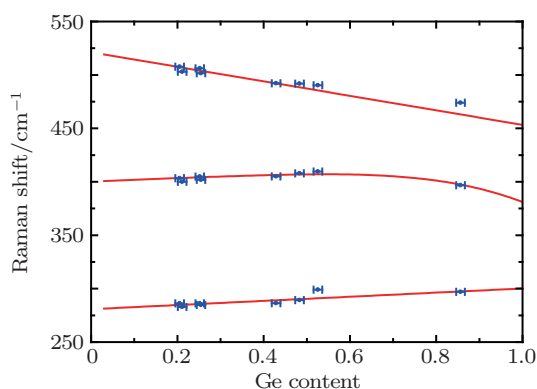

Fig. 3. (color online) Composition x-dependent frequencies for the three optic modes in the SiGe layer on SOI. The solid lines represent the fits of the data points in the fully relaxed $Si_{1-x}Ge_x$ alloy system as reported in Refs. [24] and [25].

In order to further verify the strain relaxation in the SiGe layer, the surface morphologies of the samples after the removal of surface oxide layer are measured by AFM. For the as-grown sample, a very rough surface with small SiGe islands that are distributed randomly over the surface can be observed due to the fact that the 100-nm $Si_{0.58}Ge_{0.42}$ epilayer exceeds the critical thickness (~ 25 nm) of $Si_{0.58}Ge_{0.42}$ on Si. In the Ge condensation process, the SiGe islands grow and the root-mean-square (RMS) values of the samples increase linearly with oxidation time, which is shown in Fig. 4. However, the cross-hatch patterns, commonly observed in SGOI/GOI surfaces, are not observed in the samples by the AFM. It indicates that the strain relaxations in the SiGe layers are mainly contributed to by the formation of the undulation scale of the SiGe islands.
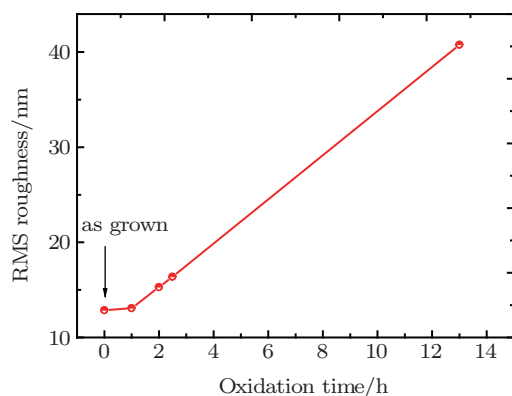

Fig. 4. (color online) Plot of the RMS roughness of the samples versus oxidation time.

Transmission electron microscopy imaging of the sample D (see Fig. 5) reveals that the non-homogeneous SiGe

layer is formed in a lengthy Ge condensation process. However, the clear lattice image with few defects can be observed in the local high-resolution transmission electron microscopy (HRTEM) imaging with 25-nm SiGe layer, and the 25-nm SGOI is uniform with a clear and sharp interface between BOX and top SiO_2. Planar defects, stacking faults and misfit dislocations, such as microtwins and 60° perfect dislocations, are not observed within the field of view. It is worth noting that the top SiO_2 layer has surface undulation while the SiGe layer underneath has observable undulation only at the interface between the top SiO_2 layer and the SiGe layer. What is more, the thicker the top SiO_2 layer is developed (marked by the black double arrow in Fig. 5), the thinner the SiGe layer underneath is formed. It reveals that the oxidation rate is increased to form a thicker SiO_2 layer at the inflection points of the corrugated SiGe film morphology.
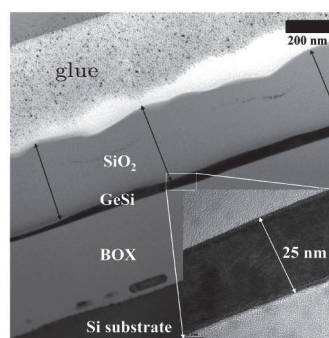

Fig. 5. HRTEM images of the sample D. The 25-nm SGOI is uniform with a clear and sharp interface between BOX and top SiO_2.

With those experimental data, a model of the non-homogeneous SiGe layer formation process is proposed as schematically shown in Fig. 6. For an as-grown sample, 100-nm $Si_{0.58}Ge_{0.42}$ epilayer on SOI wafer is above the critical thickness (~ 25 nm), the energy of the strain stored in the film becomes so large that it must be released by modifying the surface morphology that forms three-dimensional islands. Considering that the annealing process before oxidation maintains a uniform distribution of Ge atoms in the SGOI layer, it is reasonable to assume that the oxidation rate of the undulation surface is uniform at the first oxidation. However, for further oxidation, the piling up of Ge atoms at the inflection points of the corrugated SiGe film morphology is more likely to happen, and Ge accumulation in these localized regions due to its thinner thickness could lead to a higher Ge content than in other regions. Then Si atoms diffuse to the higher Ge content regions (at the inflection points of the corrugated SiGe film morphology) to lower the content gradient rather than self-limited oxidation which happens in the case of the flat surface morphology without lateral Si atoms diffusion. In other words, more Si atoms will be oxidized at the inflection points of the corrugated SiGe film morphology. Thus at the inflection points of the corrugated SiGe film morphology,

the formed SiO$_2$ layer will be thicker while the SiGe layer underneath will be consumed and become thinner. Finally, the non-homogeneous SGOI is formed.
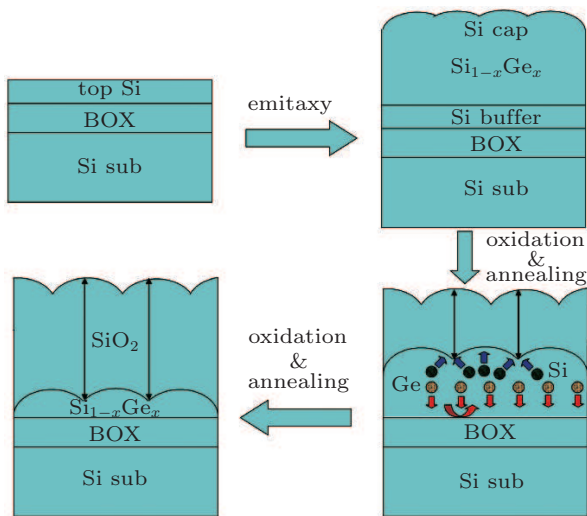

Fig. 6. (color online) Schematic illustration of the model of the non-homogeneous SiGe layer formation process.

4. Summary

We investigated Ge condensation process of a sandwiched structure of Si/SiGe/Si on a silicon-on-insulator (SOI) substrate. The strain relaxation in the SiGe layer is dominated by the formation of the undulation scale of the SiGe islands in the Ge condensation process. The non-homogeneous SiGe layer is formed due to an increased consumption of the Si atoms at the inflection points of the corrugated SiGe film morphology. The non-homogeneous SiGe layer exhibits a single crystalline nature with perfect atom lattice by TEM measurements. This insight establishes a compelling evidence that the non-homogeneous SiGe layer is formed due to the rough surface of the sample. The results are important for fabricating the SGOI and GOI substrates by Ge condensation technology for the application of Si-based devices.

References

[1] Liu J, Kimerling L C and Michel J 2012 *Semicond. Sci. Technol.* **27** 094006
[2] Yamamoto K, Ueno R, Yamanaka T, Hirayama K, Yang H, Wang D and Nakashima H 2011 *Appl. Phys. Express* **4** 051301
[3] Soref R 2006 *IEEE J. Sel. Top. Quantum Electron.* **12** 1678
[4] Wu Z, Wang C, Yan G M, Liu G Z, Li C, Huang W, Lai H K and Chen S Y 2012 *Acta Phys. Sin.* **61** 186105 (in Chinese)
[5] Huang S, Li C, Chen C Z, Zheng Y Y, Lai H K and Chen S Y 2012 *Acta Phys. Sin.* **61** 036202 (in Chinese)
[6] Taraschi G, Pitera A J and Fitzgerald E A 2004 *Solid-State Electron.* **48** 1297
[7] Nakaharai S, Tezuka T, Hirashita N, Toyoda E, Moriyama Y, Sugiyama N and Takagi S 2009 *J. Appl. Phys.* **105** 024515
[8] Tezuka T, Sugiyama N and Takagi S 2001 *Appl. Phys. Lett.* **79** 1798
[9] Bedell S, Fogel K, Sadana D and Chen H 2004 *Appl. Phys. Lett.* **85** 5869
[10] Di Z, Chu P K, Zhang M, Liu W, Song Z and Lin C 2005 *J. Appl. Phys.* **97** 064504
[11] Balakumar S, Lo G Q, Tung C H, Kumar R, Balasubramanian N, Kwong D L, Ong C S and Li M F 2006 *Appl. Phys. Lett.* **89** 042115
[12] Shimura T, Shimizu M, Horiuchi S, Watanabe H, Yasutake K and Umeno M 2006 *Appl. Phys. Lett.* **89** 111923
[13] Wang G H, Toh E H, Foo Y L, Tung C H, Choy S F, Samudra G and Yeo Y C 2006 *Appl. Phys. Lett.* **89** 053109
[14] Huang W Q and Liu S R 2004 *Chin. Phys.* **13** 1163
[15] Huang W Q, Wang H X, Jin F and Qin C J 2008 *Chin. Phys. B* **17** 3753
[16] Balakumar S, Peng S, Hoe K M, Agarwal A, Lo G Q, Kumar R, Balasubramanian N, Kwong D L and Tripathy S 2007 *Appl. Phys. Lett.* **90** 032111
[17] Gunji M, Marshall A F and McIntyre P C 2011 *J. Appl. Phys.* **109** 014324
[18] Zhang Y, Cai K, Li C, Chen S, Lai H and Kang J 2009 *J. Electrochem. Soc.* **156** H115
[19] Hu M, Li C, Xu J F, Lai H K and Chen S Y 2011 *Acta Phys. Sin.* **60** 078102 (in Chinese)
[20] Huang S, Lu W, Li C, Huang W, Lai H and Chen S 2013 *Opt. Express* **21** 640
[21] Hellberg P E, Zhang S L and Petersson C 1997 *J. Appl. Phys.* **82** 5773
[22] Tsang J, Mooney P, Dacol F and Chu J 1994 *J. Appl. Phys.* **75** 8098
[23] Chen Y, Li C, Lai H and Chen S 2010 *Nanotechnology* **21** 115207
[24] Shin H, Lockwood D and Baribeau J M 2000 *Solid State Commun.* **114** 505
[25] Perova T S, Wasyluk J, Lyutovich K, Kasper E, Oehme M, Rode K and Waldron A 2011 *J. Appl. Phys.* **109** 033502